Synthesis and Characterization of Magnetic Zeolite A for Removal of Methylene blue from Textile wastewater

S. Alaya-Ibrahim[a,b]., A.S. Kovo[a,b]., A.S. Abdulkareem[a,b]., O.D. Adeniyi[b]. M.D. Yahya[b]

[a]Nanotechnology Group, Centre for Biotechnology and Genetic Engineering, Federal University of Technology, PMB 65 Minna, Niger State, Nigeria;

[b]Chemical Engineering Department, Federal University of Technology, PMB 65, Minna, Niger State, Nigeria.

Abstract

In this research work, zeolite A was synthesized from Nigerian kaolin and FeONPs was doped onto its surface using biosynthesis route with mango leaves extract as the reducing agent. Both synthesized adsorbents were characterized using XRD, TEM, FTIR and BET surface analyser. The TEM results showed that the spherical FeONPs were well dispersed onto the surfaces of cubic shape of synthesized zeolite A, the surface area of SZA increased from 119. 98 m^2/g to 517.50 m^2/g after doping with FeONPs and the FTIR results showed that phenolics compound in the mango leaves extract might be responsible for the bio reduction of iron salt to FeONPs. The adsorption studies of MB onto both SZA and MZA increased with contact time, adsorbent dosage and temperatures. Isothermal models indicated that Langmuir, Freundlich and Temkin models can be used to describe the adsorption studies and it conformed to pseudo-second order kinetics. The thermodynamic studies showed spontaneous reaction which were endothermic in nature.

Keywords*: Local textile wastewater, magnetic zeolite A, characterization, biosynthesis*

Introduction

Over the last few decades, the level of awareness of the general public on the issues of environmental protection has increased immensely. From studies, dyes, pigments, organic pollutants and heavy metals are common pollutant present in the effluent of some industrial wastewater such as textiles, leathers, papermaking, plastics, food, rubber and cosmetics (Ghoreishi and Haghighi, 2003). Among these, textile industries have been the worst contributors of environmental pollution (Janganathan *et al*., 2014). For instance, about 9 % or (40,000 tonnes) of the overall amount of 450,000 tonnes dyestuffs produced in the world are discharged in textile wastewater (Ogugbue and Sawidis, 2011). Due to this fact, colour/dye removal from wastewater has become a great concern (Ben *et al*., 2012). Moreover, their presence and accumulation are highly toxic and has drastic effect on the environment (Couto, 2009).

Methylene blue is a basic dye which is mostly used in textile industry. This affects the water environment considerable even in small amount due to its visibility and can cause nausea, stomach upset & diarrhoea in human (Abechi, 2013). It also has the ability to reflect sunlight, thus, altering

the process of photosynthesis in plant and affect the growth of bacteria (San *et al*., 2016). Thus, most countries require factories to treat textile effluent before it is dumped so as to monitor the quality of water and reduces the threat pose by pollution (Elango *et al*., 2017).

Magnetic nanoparticles usually contain iron oxides, although, other elements may be present. The iron oxides mostly used in the field of magnetic nanoparticles are magnetite (Fe_3O_4), maghemite (y-Fe_2O_3), hematite($\propto -Fe_2O_3$), wustite (FeO), $\varepsilon - Fe_2O_3$, $\beta - Fe_2O_3$. Among which magnetite and maghemite are the very promising and popular candidate because, their biocompatibilities have already been proven (Cornell and Schwertmann, 2003).

Zeolites are low cost adsorbents which exhibit some advantages due to their ion exchange capacity, adsorbing, catalytic and molecular sieving capacities (Roehi *et al*., 2005; Faghihian and Robert, 2005). They also contain water molecules, alkali and alkaline earth metals in their framework which make them potentially useful as adsorption minerals on the contaminated surface and ground water (Thiruvenkatachari *et al*., 2008). More so, they work as a good material for nanoparticles support and hosting due to their well-defined structures and microporous cavities (Kaya *et al*., 2013; Yamaura and Fungaro, 2013)

In this study, magnetite (FeONPs) was doped on the surface of zeolite A developed from Nigerian kaolin using biosynthesis route for removal of methylene blue dye from local textile wastewater

2. Materials and Methods

2.1 Materials

The $FeCl_3.6H_20$ and $FeCl_2.4H_20$ used in this work are of analytical grade, manufactured by BDH, England. Distilled and deionized water were used throughout the study and the mango leaves was collected from Tunga area of Minna, Niger state, Nigeria.

2.2 Collection, Beneficiation and Metakaolinization of raw kaolin

The raw kaolin used in this work was collected from Ahoko, Kogi state of Nigeria. The various processes involved in the beneficiation and metakaolinization has been discussed in our previous work as represented in Figure 1.

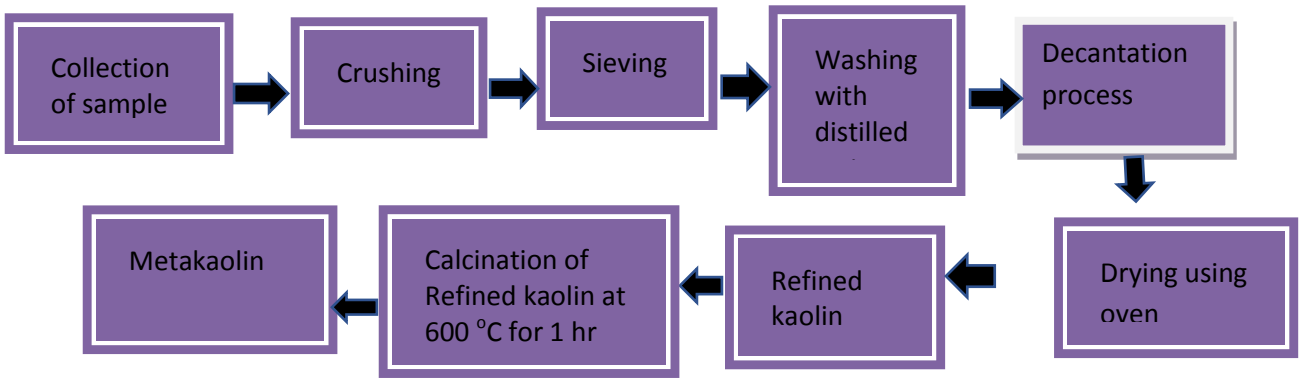

Figure 1. Block representation of Beneficiation and Metakaolinization of kaolin

2.3 Synthesis of Zeolites A from metakaolin

Zeolite A was synthesised by adding 2.85 g of metakaolin into the NaOH solution consisting of 3.3 g of NaOH pellets and 30 ml of distilled water. The resulting gel was aged for 6 hrs at room temperature on a magnetic stirrer and crystallized using a stainless autoclave in an oven at 100 ^oC for 90 mins reaction time. The crystallized product was allowed to cool, washed severally with distilled water until the pH of filtrate was 7. The sample was dried in an oven at 80 ^oC for 3 hrs and the reaction products was analysed using X-ray Diffraction (XRD), Higher Resolution Transmission

Electron Microscope (HRTEM), Fourier Transform Infrared Transmission (FTIR) and Braunauer Emmet Teller (BET) surface analysis.

2.4 Preparation of Mango Leaves Extract

20 g of crushed mango leaves was boiled in 200 ml of deionized water for 15 mins. The mixture was allowed to cool and centrifuged at 6600 rpm for 30 mins, it was decanted, filtered using Whattman filter paper. The filtrate was collected as the mango leaves extract and stored in a bottle at a temperature of 4 ^{o}C for further experimental use.

2.5 Synthesis of iron oxide nanoparticles (FeONPs)

0.324 g of $FeCl_3$ and 0.199 g of $FeCl_2.4H_20$ (ratio 2:1) were weighed with the aid of a digital weighing balance and dissolved in 100 ml of deionized water to prepare 0.01 M. 6.7 ml of the mango leaves extract was measured and poured into 5 ml of the 0.01 M of the aqueous iron chlorides prepared. This sample was kept in a water bath shaker at a temperature of 45.7 ^{o}C for a period of 11.7 mins and UV analysis was used to confirm the formation of the FeONPs. The sample was then dried at 60 ^{o}C for 4 hrs and taken for XRD, TEM and FTIR analysis.

2.6 Synthesis of Magnetic Zeolite A

A mass of 3.3 g of zeolite A was dispersed in 30 ml of distilled water and stirred for 10 mins, then 5 ml of prepared $FeCl_3$ and $FeCl_2$ (2:1) was added to the suspension under vigorous stirring for 30 mins at a temperature of 45.7 ^{o}C. 6.7 ml of mango leaves extract was added while still vigorously stirred for another 11.7 mins. The mixture was then centrifuged at 6000 rpm for 30 mins, washed and dried in an oven for 2 hrs. The product was analysed using Braunauer Emmet Teller (BET), FT-IR, XRD and TEM.

2.7 Characterization of Adsorbents

The microstructure and sizes of the synthesized zeolites A were determined using Zeiss Auriga High Resolution Transmission Electrons Microscopy **(**HRTEM) with 54 µA emission current, 3950 V and spot size of 3mm. The sample was prepared by suspending 0.02 g of adsorbents in 10 ml of methanol which was ultra- sonicated until there was complete dispersion of the adsorbents. A drop of the slurry was dropped on the holey carbon grid and photo light was used to dry the sample. The dried sample was loaded onto the sample holder and the electron microscope was operated for imaging. The phase identification and crystalline nature of the synthesized adsorbents was done using Bruker AXS D8 X-ray diffractometer. This was done by crushing 1000 mg of the sample to determine the average bulk composition, followed by the preparation of the powdered sample with the aid of sample preparation block. the sample was then compressed and placed in a sample holder which was later mounted on the x-ray diffraction cabinet. Braunauer Emmet Teller (BET) analysis was used in determination of the surface area of the synthesized adsorbents using Quantachrome BET analyzer of model NOVA 4200e. 0.1 g of the synthesized adsorbents was put in a tube which was degassed at 90 ^{o}C for 4 hr. The nitrogen adsorption-desorption isotherms were collected at approximately 196 ^{o}C using Micrometritics ASAP 2020 Accelerated Surface Area and Porosimetry analyser.

2.8 Collection and Dye analysis of the Textile Wastewater (TWW)

The textile wastewater used in this study was collected from local textile industry in Ilorin, Kwara state, Nigeria. The wastewater was analysed using UV-vis spectrophotometer to ascertain the types of dyes present. This was done by scanning the wastewater through the UV vis spectrophometer from range of 190-800 nm for available wavelengths and the results revealed several peaks ranging

from 195-620 nm. However, the only main peak identified was at 620.50 nm, which was attributed to methylene blue (Dhananasekaran *et al*., 2016; Chen *et al*., 2016).
In order to determine the methylene blue concentration, calibration curve was used by preparing different concentrations (0.002, 0.004, 0.006 and 0.008 g/L) of methylene blue and the absorbance in the sample was determined at wavelengths corresponding to 620.50 nm.

2.9 Adsorption studies

Batch adsorption study was employed in evaluating the rate and equilibrium data. Equilibrium isotherms were obtained by studying the adsorption process of synthesized zeolite A (SZA) and magnetic zeolite A (MZA) at different contact time, temperature and adsorbent dosage. The effect of contact time was studied by varying the contact time of adsorbents with the textile effluent at 1, 3, 5, 10, 20, 30, 40, 50, 60, 90, 120 and 150 mins in order to establish the adsorption equilibrium. Effects of temperature was studied at 30, 40, 50 and 60 ^{o}C so as to evaluate the adsorption thermodynamics parameters and effects of adsorbent dosage were also investigated from 0.5-2.0 g at 0.5 g intervals to investigate adsorption isotherms. All these were done on the Textile wastewater using SZA and MZA at a temperature of 30 ^{o}C except those studies in which temperatures were studied. The initial and final concentration of the MB in the textile wastewater were determined using UV-spectrophotometer. Equilibrium adsorption of the textile effluent was performed by shaking 2 g of adsorbent in 100 ml of the textile effluent. This was placed in a shaker at a temperature of 30 ^{o}C and speed of 200 rpm for a period of 90 mins. Adsorption equilibrium and percentage removal were calculated using the relationship as thus;

$$q_e = \frac{C_o - C_e}{m} \times V \quad (1)$$

$$\%\ removal = \frac{C_o - C_e}{C_o} x100 \quad (2)$$

q_e is the amount of MB adsorbed at equilibrium (mg/g), C_o, initial MB concentration in (mg/L), C_e, concentration of MB at equilibrium (mg/L), m is the mass of adsorbent (g) and V, volume of the solution (mL)

2.11 Adsorption Isotherm

The adsorption isotherm model used in describing the adsorption process in this present study are Langmuir, Freundlich, and Temkin isotherms.
Langmuir Isotherm is based on the postulation that there is formation of single layer of the adsorbate onto the exterior surface of the adsorbent, after which there will be no further adsorption. Hence, there is equilibrium distribution of the contaminants between the solid and the liquid phase (Wang *et al*., 2014; Langmuir, 1916). This can be illustrated as:

$$qe = \frac{q_m\, k_a\, C_e}{1 + kC_e} \quad (3)$$

Equation can be linearized in this form;

$$\frac{Ce}{q_e} = \frac{C_e}{q_m} + \frac{1}{K_a q_m} \quad (4)$$

where q_e is the quantity of MB adsorbed (mg/g), C_e is the equilibrium concentration of the MB (mg/L), q_m and K_a are the Langmuir constant related to the maximum adsorption capacity (mg/g) and energy of adsorption (L/mg) respectively. The values of q_m and K_a can be estimated from the slope and intercept of plots of $\frac{Ce}{q_e}$ against C_e. In addition, an imperative characteristic of the Langmuir isotherm can be stated with respect to dimensionless factor R_L , which is defined as;

$$R_L = \frac{1}{(1 + b(C_0))} \quad (5)$$

The R_L value indicates the type of adsorption as unfavourable ($R_L > 1$), linear ($R_L = 1$), favourable ($0 < R_L < 1$) or irreversible ($R_L = 0$). R_L *is* the dimensionless constant separation factor, b, Langmuir adsorption constant related to the affinity of the binding sites in L/mg, C_0, liquid- phase initial concentration of contaminants in mg/L. The Freundlich Isotherm is basically used to describe the binding of adsorbates onto heterogeneous surfaces as well as the adsorption of many layers and it is expressed as;

$$qe = k_f Ce^{1/n} \quad (6)$$

and can be linearized in the form;

$$log\, q_e = log\, K_f + \frac{1}{n} log C_e \quad (7)$$

where q_e is the amount adsorbed at equilibrium (mg/g), K_f is the Freundlich constant, 1/n is the heterogeneity factor, K_f and 1/n are linked to the capacity and the intensity of the adsorbent, C_e is the equilibrium concentration (mg/L). The values of K_f and $\frac{1}{n}$ can be obtained from the slope and intercept of the plot of $log\, q_e$ vs $logC_e$ (Freundlich , 1906). Temkin Isotherm is based on indirect effect of interactions between an adsorbate and another adsorbate on the surface of the adsorbent. The heat of adsorption of all molecules is also assumed to diminishes in a linear form due to the increment of the surface coverage (Dada *et al*., 2012). The linear form of Temkin is given as;

$$q_t = \frac{Rt}{b}\, lnk_t + \frac{Rt}{b} lnC_e \quad (8)$$

b and k_t are the Temkin constants related to the heat of adsorption (J/mol) and number of contaminants adsorbed (L/g) respectively. These are obtained from the slopes and intercepts of plots of q_t against ln C_e

2.11 Adsorption Kinetics

In order to examine the mechanism of adsorption of MB onto the synthesized adsorbents, the characteristic constants of adsorption were evaluated using pseudo-first order equation of Lagengren and pseudo-second order kinetic models as expressed in equations 9-11

$$\log(q_e - q_t) = \frac{1}{q_e} - {}^{k_1}/_{2.303}\, t \quad (9)$$

k_1 is the pseudo-first order rate constant in (min^{-1}). If a Pseudo- first order model applies, then a reversible reaction occurs in the process which is recognised by the existence of equilibrium between the contaminants and the adsorbents (Radnia *et al*., 2011). Pseudo-second order equation is generally expressed linearly as (Yakout and Elsharif, 2010);

$$\frac{t}{q_t} = \frac{1}{k_2 qe^2} + \frac{1}{q_e} t \quad (10)$$

q_e and q_t are the amounts of adsorbates adsorbed at equilibrium and time (t) respectively, k_2 and r_i are the pseudo-second order constant in (g/mg.min) and (mg/g.min) respectively, where;

$$r_i = k_2 qe^2 \quad (11)$$

If pseudo-second model applies, a straight-line graph through which the slopes and intercept evaluated from it gives the constants, then chemisorption is the rate limiting step of the sorption process (Radnia *et al*., 2011).

2.7 Thermodynamics of Adsorption

The spontaneity of the sorption of the adsorbates-adsorbents can be assessed through thermodynamic parameters such as enthalpy change (ΔH^o), Gibb's free energy (ΔG^o) and entropy change (ΔS^o). Any reaction where (ΔH^o) and (ΔG^o) are negative whereas (ΔS^o) is positive implies a spontaneous reaction (Margata *et al*., 2013). Thus;

$\Delta G^o = \Delta H^o - T\Delta S^o$ (12)

$lnK = \frac{\Delta S^o}{R} - \frac{\Delta H^o}{RT}$ (13)

ΔH^o and ΔS^o are evaluated from the slope and intercept of the plot of lnK vs 1/T and the free energy of specific adsorption ΔG^o ($\frac{kJ}{mol}$) can be calculated using Equation 12

3.0 Results and Discussions

3.1 Characterization of Synthesized Adsorbents

Iron oxide nanoparticles was synthesised by reacting 6.73 ml of mango leaves extract with 5 ml of $FeCl_3$ and $FeCl_2$ (ratio 2:1) at 45.66 ^oC for a period of 11.7 mins. An immediate colour change from light yellow to black colour was observed indicating the formation of FeONPs and was confirmed using UV- Vis spectroscopy.

The UV spectra obtained is shown in Figure 1a, which shows a corresponding wavelength at 259 nm, thus, the colour change was due to the excitation of the Surface Plasmon Vibrations (Shah *et al.*, 2014) as a result of reduction of the iron salts by the mango leaves extract to form iron oxide nanoparticles.

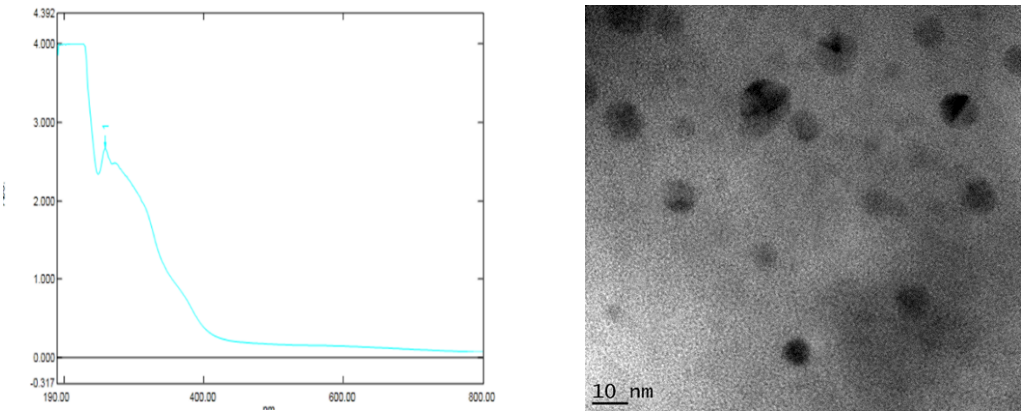

Figure 1 (a) UV-Vis Spectroscopy of Synthesised FeONPs (b) TEM Micrograph of FeONPs

In addition**,** TEM analysis was performed to further elucidate the formation of FeONPs as shown in Figure 1b. The result reveals well dispersed spherical FeONPs with an average particle size of 10.17 nm.

The XRD pattern of synthesized SZA and MZA are shown in Figure 2. The pattern reveals reflections at 7.1 ^{o}, 10.10 ^{o}, 12.4^o, 16.0 ^{o}, 21.6 ^{o}, 24 ^{o}, 26.3 ^{o}, 29.8 ^{o}, 30.7 ^{o}, 32.5 ^{o}, and 34.1 ^{o} of 2 theta corresponding to the crystallographic planes; (200), (220), (222), (420), (600), (622), (640), (644), (822), (840), (644) respectively which are the main peaks in identifying zeolite A (Treacy and Higgins, 2001). It could be observed from the figure that the intensity of the MZA peaks at 29.1^o, 32.4^o, 40.30^o, 50.14^o, 54.9^o and 60.02^o reduced as compare to the SZA. This is attributed to the incorporation of the magnetite into the SZA framework, thus leading to the reduction in their peaks (kamya *et al*., 2011).

The TEM analysis of the iron oxide nanoparticles doped zeolite A (MZA) were also performed to investigate the changes in the morphology of zeolite A after doping with FeONPs as shown in Figure 3.

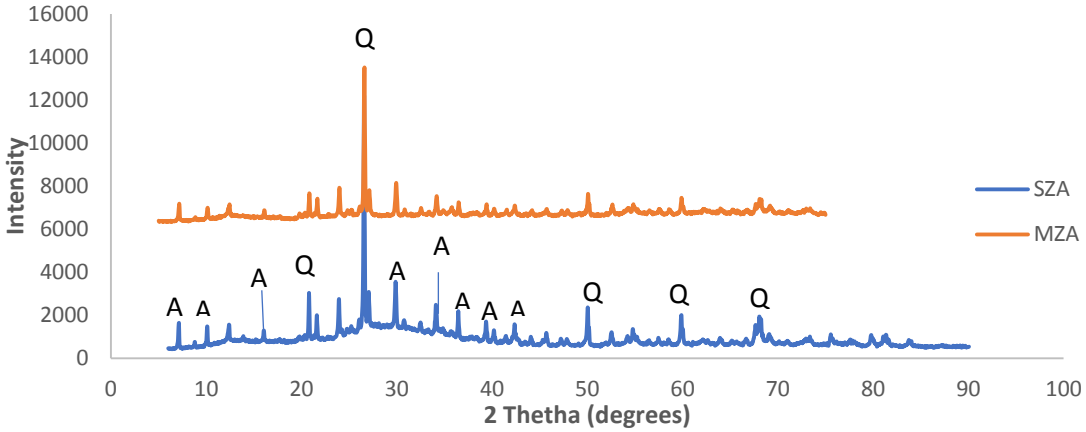

Figure 2. XRD Pattern of SZA and MZA

The micrographs revealed the cubic nature of synthesised zeolite A as shown in Figure 3a while Figure 3b shows that the SZA were covered by the FeONPs as indicated by the black spherical patches, which is an attribution of the nanoparticles. It can also be noticed that the FeONPs are clustered on the SZA surface. This might be due to the magnetic nature of FeONPs, thereby, making the particles agglomerated as a result of attraction between the particles and the SZA. However, the FeONPs are well dispersed on the surface of zeolite A.

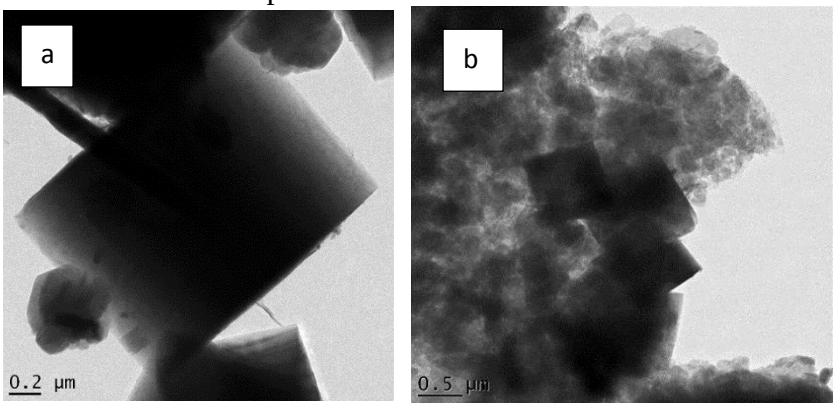

Figure 3. TEM images of (a) SZA and (b) MZA

BET analysis was performed in order to assess the effect of doping on the surface area of the SZA and the result is presented in Table 1. The results suggested that the FeONPs greatly affected the surface area and the pores of SZA as the surface area increased from 119.98 m^2/g to 517.50 m^2/g and the pores from 3.28 nm to 6.32 nm. Thus, they are mesoporous in size according to IUPAC classification of pore size; < 2nm= micropores, 2-50 nm = mesoporous and > 50 = macropores. Also, MZA with higher pore diameter and total pore volume implies higher porosity and number of pores respectively.

Table 1: BET analysis of synthesized Adsorbents

	SZA	SDZA
BET surface area (m^2/g)	119.98	517.50
Pore diameter (nm)	3.28	6.32
Total pore volume(cc/g)	0.039	0.185

The FTIR of SZA and MZA were performed to study the effect of the synthesized nanoparticles on the surface of SZA as shown in Figure 4. The IR spectrum of SZA (Figure 4 a) reveals bands at 3698 – 3622 cm^{-1} which is attributed to the hydrogen group of water molecules present in the pores of zeolite A, while that at 1652 cm^{-1} with sharp and low intensity band correspond to the bending vibration of water. The sharp peak around 1000 cm^{-1} correspond to the asymmetric stretching vibrations of all zeolitic materials (Gougazeh and Buhl, 2014; Byrappa and Kumar, 2007). The absorption band at 694 cm^{-1} is associated with symmetric stretching of T-O-T vibrations of sodalite framework which is in good agreement with 693 cm^{-1} reported by Gougazeh and Buhl (2014) for hydrosodalite zeolite. The spectrum at 776 cm^{-1} was due to the external linkage tetrahedral regions of the sodalite (Byrappa and Kumar, 2007).

The spectra of MZA as revealed in Figure 4b shows the same spectra pattern with SZA (see Figure 4a) except for an additional band noticed at 2891 cm^{-1}. This is attributed to the carboxyl group present on the surface of the nanoparticles. More so, the decrease in the intensities of peaks as observed in MZA in Figures 4b as compared to SZA in Figure 4a indicated the successful doping of the nanoparticles in the framework of the zeolite A. This results further supports the XRD results which showed reduction in the intensities of the peaks of MZA as compared to SZA

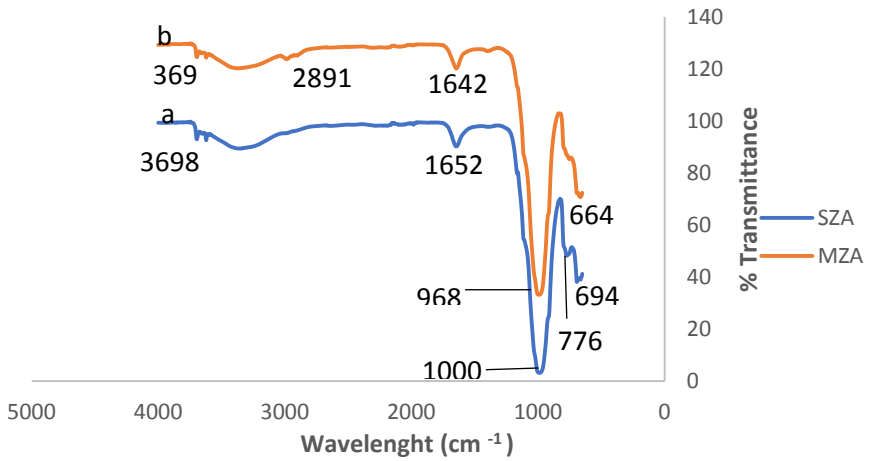

Figure 4. FTIR of SZA and SDZA

3.2 Analysis of Local Textile Wastewater

In order to ascertain the different types of dyes present in wastewater, UV analysis was performed and the results is presented in Figure 5

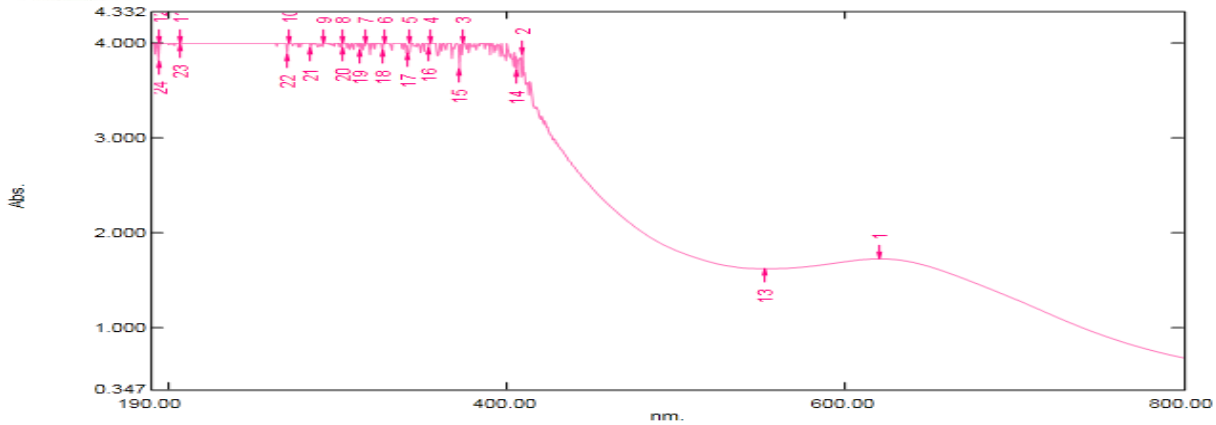

Figure 5. UV -Vis Spectrum of Local Textile Wastewater

According to the UV result as shown in Figure 5, the only main peak identified is at 620.50 nm, which was attributed to methylene blue (Dhananasekaran *et al*., 2016; Chen *et al*., 2016). Other bands were observed between 195nm and 409 nm. The band at 354-409 nm and 291-328 nm were attributed to violet colour (Jakub, 2018) and sulphate (Liang *et al*., 2006). This may be as a result of the raw materials such as sulphate, soda ash and dyes used in the local textile industry. This prompt the use of MB as the main indicator in the present study.

3.2.1 Effects of Contact Time on Removal of Methylene Blue

The effects of contact duration between the textile effluent and the synthesised adsorbents were investigated for removal of MB over a period of 1, 3, 5, 10, 20, 30, 40, 50, 60, 90, 120 and 150 mins at 30 ^{o}C, adsorbent dosage of 1.0 g in 50 ml of textile effluent. The results are presented in Figure 6. According to Figure 6, the removal of MB increased with increase in contact time for both SZA and MZA until equilibrium, when it began to diminish (Rahman and Akter, 2016; Yusuf-Alaya, 2014; Ponnusami *et al*., 2009).

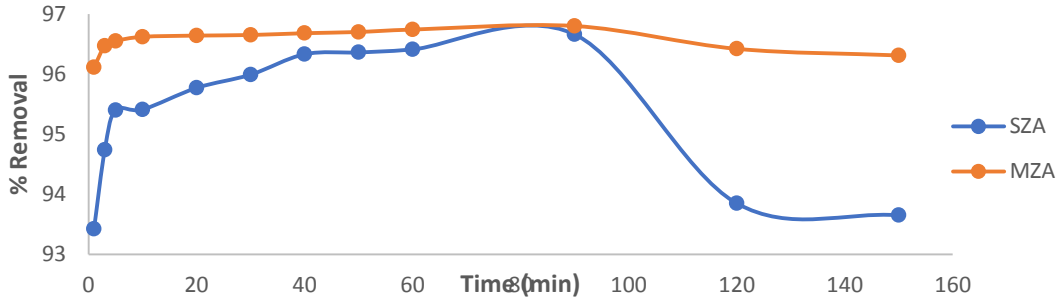

Figure 6. Effects of Contact Time on Removal of MB

The equilibrium was achieved at 90 mins suggesting that the surfaces of the adsorbents were saturated thereby reducing the binding force between the MB and the adsorbents. This in turn reduced the rate of adsorption. Also, the presented results revealed that the MB removal was rapid from the first minute of contact with the adsorbents, removing 93.42 % and 96.11 % for SZA and MZA respectively. This is an evidence that there was proper contact between the MB and the adsorbents (Rahman and Akter, 2016). The removal of MB by MZA was observed to be higher than SZA, which is expected due to their surface area as revealed by BET analysis.

3.2.2 Effect of Adsorbent Dosage on Removal of MB

The effect of adsorbent dosage on the removal of MB were also studied and the result as illustrated in Figure 7 show that the removal of MB from textile effluent increased with increase in adsorbent dosages for both adsorbents. The reason might be that when the adsorbent quantity was small in the solution, there was minimal active sites for binding unto their surfaces, thus, the number of active sites increased with increase in the adsorbent quantity. Thereby, increasing the percentage removal of MB from 94-96 % and 96-98% by SZA and MZA respectively. Similar result was obtained by Rahman and Akter, when they used chitin to remove dyes from TE, 96-97 % removal was also achieved (Rahman and Akter, 2016).

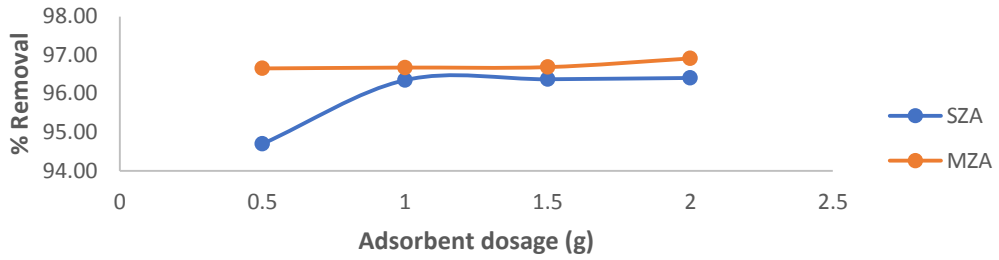

Figure 7. Effects of Adsorbent dosage on Removal of MB

3.2.3 Effects of Temperature on the removal of MB

The temperature effects on the removal of MB from TE using the synthesized adsorbents were also investigated and the result is shown in Figure 8. The result reveals that the sorption of MB onto SZA and MZA increased with increase in temperature. The result is an indication that the force of attraction between the synthesized adsorbents and MB are of strong type and as such there was no mobility as the temperature increased causing MB molecules to be strongly attracted to the zeolites (Margeta, 2013). The results are in good agreement with the literature (Bankole *et al*., 2017; Rahman and Aktar, 2016; Yusuf-Alaya, 2014).

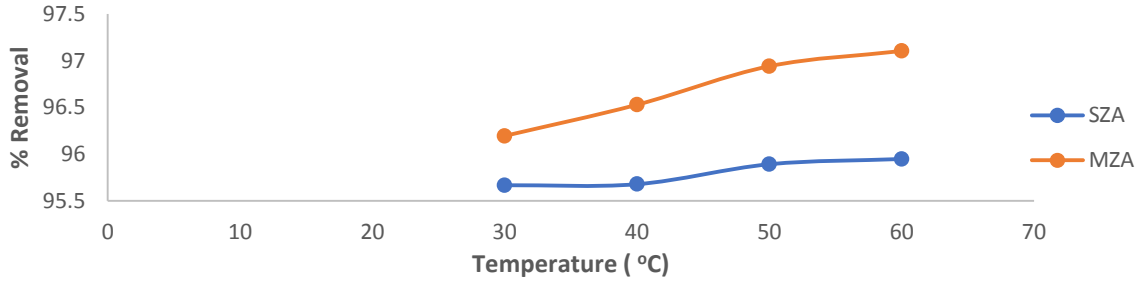

Figure 8. Effects of Temperature on Removal of MB

3.3 Adsorption Isotherms

The equilibrium relationship between the adsorbents and adsorbates were evaluated using Langmuir (Equation 4), Freundlich (Equation 7) and Temkins (Equation 8)

The Langmuir parameters are presented in Tables 2. The q_m, which is related to maximum adsorption capacity are 2.65 and 2.70 mg/g for SZA and MZA respectively. This suggest that MZA has a higher affinity for removal of methylene blue than SZA. This can be linked to MZA having the higher surface area compared to SZA as earlier stated. The Langmuir adsorption coefficient, $k_{L,}$ which is related to energy of sorption also indicated that MZA has a value of 15.29 L/g, which was higher than 9.81 L/g of SZA. The separator factor R was used in identifying the favourability of the

adsorption process, thus, when R>1 is unfavourable, R=1 is linear and 0<R<1 is favourable. From the table, the values of the separation factor R are in the range of 0 to <1, suggesting that the adsorption of MB onto the adsorbents are favourable. Both coefficient of regression R^2 are 1, confirming the monolayer coverage of the MB onto the surfaces of the adsorbents as well as their active sites been homogeneously distributed.

Table 2: Isotherm Constants for the Adsorption of MB onto SZA and MZA

Isothermal Models	SZA	MZA
Langmuir		
q_m	2.65	2.70
k_L	9.81	15.29
R	0.0081	0.0011
R^2	1	1
Freundlich		
1/n	0.0461	0.0331
k_f	0.337	0.341
R^2	1	1
Temkin		
B	$1.98x10^4$	$2.72x10^4$
k_T	$6.571x10^9$	$2.37x10^{14}$
R^2	1	1

The removal of MB onto the heterogeneous surfaces of the synthesised adsorbents were also investigated using Freundlich isothermal model and the adsorption parameters are presented in Tables 2. The values of 1/n which is related to the intensity of adsorption are in the range of zero to < 1, this suggested that they have strong surface heterogeneity since their values are close to 0. These values satisfy the condition 0>1/n<1, thus, the closer the value to zero, the stronger the surface heterogeneity (Margeta, 2013; Foo and Hameed, 2010). On the other hand, the values of k_f, which is related to the adsorption capacity of the adsorbents are 0.337 and 0.341 L/g for SZA and MZA respectively. This shows that MZA has the higher affinity for removal of MB than SZA. However, the coefficient of regression R^2 for both adsorbents are 1, depicting that sorption of MB onto both SZA and MZA fitted Freundlich isotherm model correctly; therefore, there was formation of multilayer coverage of MB on the surfaces of the adsorbents (Margeta, 2013).Temkin isotherm model provide information with respect to interaction between adsorbent and adsorbate; it also assumes that the heat of adsorption reduces with increase in surface coverage. This was tested in this study and the results as presented in Table 2. The k_T values are $6.57x10^9$ and $2.37x10^{14}$ for SZA and MZA respectively, this is an indication that strong binding force existed between the MB and the adsorbents surfaces while the values of b shows how the heat of adsorption reacted with respect to surface coverage (Dada *et al*., 2012). The obtained results show that Temkin model can be used to describe the adsorption of MB by the two adsorbents with their R^2 values of 1.

3.4. Adsorption Kinetics

The mechanism and rate controlling steps of the MB onto the synthesized adsorbents were investigated using Pseudo-first order model and Pseudo-second order model. Their various equations were earlier stated (Equations 9 and 10) and their various results are presented in Table 3. The Pseudo-first order and Pseudo-second order models were investigated in this work as presented in the Table 3. According to the table, the Pseudo-first order parameters q_e which is related to the sorption

capacity are not in agreement with the experimental values and the coefficients of regression are 0.922 and 0.7107 for SZA & MZA respectively. On the other hand, the calculated q_e values of the pseudo-second order are reasonably in agreement with experimental q_e values. Even though, the maximum adsorption capacity was observed by MZA as revealed by calculated q_e values. None the less, the coefficient of regression (R^2) values of SZA and MZA are 1. Therefore, the adsorption of MB onto the synthesized zeolites may be chemisorption in nature, thus, conformed with pseudo-second order kinetic model.

Table 3: Kinetic Constants for the Adsorption of MB onto SZA and MZA

Isothermal Models	SZA	MZA
Pseudo-first order		
k_1 (min^{-1})	2.0978	0.0283
q_e (mg/g)	0.8317	0.5027
R^2	0.922	0.7107
Pseudo-second order		
k_2 (g/mg.$min^{-0.5}$)	4.855	41.295
q_e (mg/g)cal	2.788	2.795
q_e (mg/g)exp	2.773	2.780
r_i (mg/g.min)	37.740	322.61
R^2	1	1

3.5. Thermodynamics of Adsorption

The thermodynamic parameters such as Gibb's free energy, ΔG^o, the enthalpy ΔH^o and the entropy ΔS^o were also evaluated as they represent the vital index for the practical applications of a process. The parameters were determined from the Equations 12 & 13 and the K was obtained from Equation 14;

$$K = {}^{q_t}/_{C_t} \qquad 14$$

K is the equilibrium constant, q_t (mg/g) is adsorption capacity of MB at time (t) while C_t (mg/g) is the corresponding concentrations. The plots of ln K vs 1/T is shown in the Figure 10

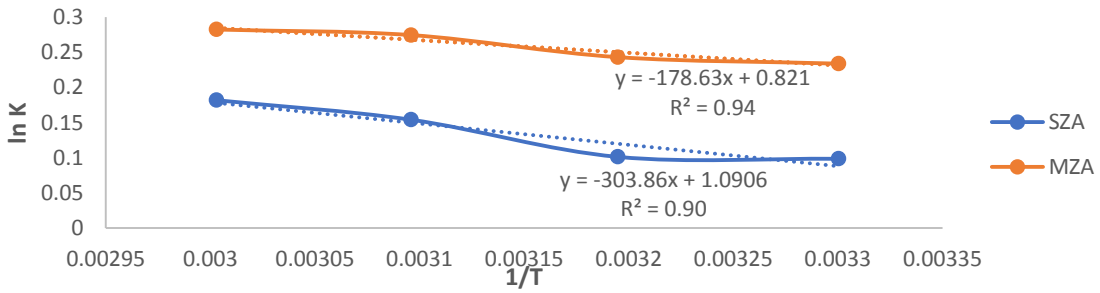

Figure 10. Plots of ln K vs 1/T

ΔH^0 & ΔS^0 were evaluated from the slopes and intercepts of the plots respectively while the ΔG^0 were calculated from the Equation 12 and tabulated in the Table 4

The results as presented in Table 4 shows that the adsorptions of MB onto SZA and MZA were endothermic reactions as indicated by their positive values of ΔH^o. This is supported by the increase in adsorption of MB with increase in temperature observed in the course of studying the effect of temperature on their adsorption capacities. However, MZA required a lower energy than SZA in

removal of MB as shown in the table, this shows that the binding force between the MZA and MB was stronger than that of SZA, which made it easier for the contaminant to be bonded on it. Also, the positive values of ΔS^o show that randomness increased at the solid- solution interface (Piccin *et al*., 2011). The negativity of ΔG^o indicated that the adsorption process of MB was spontaneous and the increase in the negativity with temperature suggested that at a higher temperature, the rate of adsorption of MB onto SZA and MZA increased (Kalavathy *et al,* 2005).

Table 4. Thermodynamic parameters of adsorption of MB unto SZA and MZA

Adsorbents	**ΔG^o (kJ/mol)**				**ΔH^o**	**ΔS^o**
	30 ^{o}C	**40 ^{o}C**	**50 ^{o}C**	**60 ^{o}C**	**(kJ/mol)**	**(J/mol)**
SZA	-0.221	-0.311	-0.402	-0.493	2.526	9.067
MZA	-0.058	-0.652	-0.719	0.788	1.485	6.826

4.Conclusion

In this research work, zeolite A was synthesized from Nigerian kaolin and FeONPs was successfully doped onto its surface using biosynthesis route with mango leaves extract as the reducing agent. Both synthesized adsorbents were characterized using XRD, TEM, FTIR and BET surface analyser. The TEM results showed that the spherical FeONPs were well dispersed onto the surfaces of cubic shape of synthesized zeolite A, the surface area of SZA increased from 119. 98 m^2/g to 517.50 m^2/g after doping with FeONPs and the FTIR results showed that phenolics compound in the mango leaves extract might be responsible for the bio reduction of iron salt to FeONPs. The adsorption studies of MB onto both SZA and MZA increased with contact time, adsorbent dosage and temperatures. Isothermal models indicated that Langmuir, Freundlich and Temkin models can be used to describe the adsorption studies and it conformed to pseudo-second order kinetics. This implies that the sorption of MB onto the surface of the synthesized adsorbents surface might either be homogeneous or heterogeneous in nature. Furthermore, the MZA have demonstrated stronger interactions with MB than SZA, which might be as a result of the incorporation of nanoparticles onto the surface of the SZA for enhancement of its surface area for better adsorption. The thermodynamic studies showed spontaneous reaction which were endothermic in nature. Thus, the synthesized adsorbents are effective in textile wastewater treatments.

5. References

Abechi, S.E. (2013). Equilibrium adsorption studies of methylene blue onto palmkernel shell based activated carbon. *International Referred Journal of Engineering and Science* 2: 38-45

Al-Ruqeishi, M.S., Mohiuddin, T., and Al- Saadi, L.K. (2016). Green synthesis of iron oxide nanorods from deciduous Omani mango leaves for heavy oil viscousity treatment. *Arabian Journal of Chemistry.* http//.dx.doi.org/10.1016/j-arabjc2016.04.003

Balamurugan, M., Saravanan, S., and Soga, T. (2014a). Synthesis of iron oxide by using Eucalyptus Globulus plant extract. *Journal of Surface Science & Nanotechnology* 12: 363-367

Bankole, M.T., Abdulkareem, A.S., Tijani, J.O, Ochigbo, S.S., Afolabi, A.S., and Roos, W.D. (2017). Chemical oxygen demand removal from electroplating wastewater by purified and polymer functionalized carbon nanotubes adsorbents. *Water Resources and Industry* 18; 33-50,

Ben Mansour, H., Houas I, Montassar, F., Ghadira, K., Barillier, D., Mosrati, R., Chkir-Ghadira, L., (2012). Alteration of invitro and acute in vivo toxicity of textile dyeing wastewater after

chemical and biological remediation. *Environmental science and pollution. Research international*; D01 10. 1007/s 11356- 012- 0802-7.

Byrappa, K and Suresh Kumar, B.V. (2007). Characterization of zeolites by Infrared spectroscopy. *Asian Journal of Chemistry* 19(6): 4933-4935.

Chen, L., Li, Y., Hu, S., Sun, J., Du, Q., Yang, X., Ji, O., Wang, Z., Wang, D. and Xia, Y. C. (2016). Removal of methylene blue from water by cellulose/graphene oxide fibres. Journal of experimental Nanoscience 11(14): 1156-1170, doi: 10.1080/17458080.2016.11a8499

Cornel, R.M. and Schwertmann, U. (2003). *The iron oxide: structures, properties, reactions, occurrences and uses.* Second Revised Edition. Wiley. VCH Verlag GmbH & Co. KGaA, Weinheim, pp 119-121

Couto, S.R., (2009). Dye removal by immobilised Fungi. Biotechnology Advances; vol.27 (3) pp. 227- 235.

Dada, A.O., Olalekan, A.P., Olatunya, A.M., and Dada, O. (2012). Langmuir, Freundlich, Temkin, and Dubinin-Radushkevich Isotherms studies of equilibrium sorption of Zn^{2+} unto phosphoric acid modified rice husk. *Journal of Applied Chemistry* 3(1):38-45

Dhananasekaran, S., Palanivel, R., and Pappu, S. (2016). Adsorption of methylene blue, bromophenol blue and coomassie brilliant blue by 2. Chitin nanoparticles. *Journal of Advanced Research* 7 (1): 113-124, doi. 10.1016/j.jare.2015.03.003

Elango, G., Rathika, G., and Elango, S. (2017). Physicochemical parameters of textile dyeing effluent and its impact with casestudy. *International Journal of Research in Chemistry and Environmen*t 7(1): 17-24.

Foo, K.Y. and Hameed, B.H. (2010). Insight of the modelling of adsorption isotherm systems. *Chemical Engineering Journal* 156:2-10, doi: 10.1016/j.cej.2009.09.013

Freundlich, H.M.F., (1906). Over the adsorption in solution; *Journal of Physical Chemistry* 57:385-470.

Ghoreishi, M., and Haghighi, R., (2003). Chemical catalytic reaction and biological oxidation for treatment of non-biodegradable textile effluent. *Chemical Engineering Journal* 95:163-169

Gougazeh, M. and Buhl, J.C. (2014). Synthesised and characterization of zeolite A by hydrothermal transformation of natural Jordanian kaolin. *Journal of Association of Arab Universities for Basic & Applied Sciences* 15: 35-42

Jaganathan, V., Chereruveetil, P., Chellasamy, A., Premapriya, M.S. (2014). Environmental pollution of risk analysis and management in textile industry: A preventive mechanism. *European Scientific Journal* 2:1857.Jakub, M. (2018). Difference between violet and purple.

Kalavathy, M.H., Karthikeyan,T., Rajgopal, S., Miranda, L.R., (2005). Kinetic & Isotherm studies of Cu (II) adsorption onto H_3PO_4 – activated rubber wood sawdust. Journal of Colloid Interface Science; pp 292- 354

Kamyar, S., Mansor, A., Mohsen, Z., Wan Md Zin, W.Y., and Nor. A.J. (2011). Fabrication of siver nanoparticles doped in the zeolite framework and antibacterial activity. *International Journal of Nanomedicine* (6): 331-341, doi:10.2147/IJN.S16964

Kaya, E.M.O., Ozean, A.S., Gok, O., Ozean, A., (2013). Adsorption kinetics and isotherm parameters of Naphthalene onto Natural and Chemically Modified Bentonite from Aqeous Solutions. *Adsorption* 19, 879- 888.

Langmuir, I. (1916). The adsorption of gases on plane surface of glass, mica and platinum, *Journal of American Chemical Society* 40: 1361-1368.

Liang, Li., Xian, Z., Xun, S. and Xueqin, S. (2006). Sulphate may play an important role in the wavelength dependence of laser induced length. Optical Society of Analics 14 (25) 12196-12198

Margata, K., Logar, N.Z., siljeg, M and Farkes, A. (2013). A natural zeolite in water treatment-

How effective is their use. *INTECH* Chapter 5; 81-111, http://dx.doi.org/10.5772/50738

Meyyappan, A., Banu, S.A. and Kurian, G.A. (2015). One step synthesis of iron oxide nanoparticles via chemical and green route- an effective comparison. *International Journal of Pharmacy and Pharmacy Sciences* 7(1): 70-74

Ogugbue, C.J., Sawidis T., (2011). Bioremediation and Detoxification of Synthetic Wastewater Containing Triarylmethane Dyes by Aeromonas hydrophila Isolated from Industrial Effluent. Biotechnology Research International; DOI 10.4061/2011/967925

Piccin, J.S., Dotto, G.L., Vierra, M.L.G. and Pinto, L.A.A. (2011). Kinetic and mechanism of the dye FD& C Red 40 binding onto chitosan. *Brazilian Journal of Chemical Engineering* 28(2): 295- 304. Retrieved on January 10th, 2018 from http://www.repositorio.furg.br/bitstream/handle/1/4602/31-%20ADSORPTION%20ISOTHERMS%20AND.pdf? sequence=1

Radnia, H., Ghoreyshi , A. A., and Younesi, H. (2011). Isotherm and kinetics of Fe (II) adsorption onto chitosan in a batch process. *Iranica Journal of Energy & Environment* 2(3):250 – 257,

Rahman, F.B.A and Aktar, M. (2016). Removal of dyes from textile wastewater adsorption using shrimpshell. *International Journal of Water Resources* 6:244, doi:10.4172/2252-5211.1000244

San, S.E., Adeeyo, O.A., Efeovbokhen, V., Ojewumi, M., Ayoola, A. and Ogunbiyi, A. (2016). Comparative analysis of adsorption of methylene blue dye using carbon from palm kernel shell activated by different actively agents. *3rd International Conference on African Development* Issues (CU-ICADI 2016); 176-181

Shah, S., Daggupta, S., Chakraborty, M., Vadakkekara, R., and Hajoori, M. (2014). Green synthesis of iron nanoparticles using plant extracts. *International Journal of Biological and Pharmaceutical Research* 5(6):549-552. Retrieved from www.ijbpr.com

Treacy, M.M.J. and Higgins, J.B. (2001). *Collection of simulated XRD powder patterns for zeolites*, fourth edition, Elsevier, New York.

Thiruvenkatachari, R., Vigneswaran, S., Naidu, R., (2008). Permeable reactive barrier for groundwater remediation. *Journal of Industrial Engineering Chemistry*, 14 145- 156.

Wang, T., Lin, J., Chen, Z., Megharaj, M., and Naidu, R., (2014). Green synthesised Iron nanoparticles by green tea and eucalyptus leaves extracts used for removal of nitrate in aqeous solution. *Journal of Cleaner Production* 83: 413-419

Yakout, S.M. and Elsherif, E. (2010). Batch kinetic, isotherm and thermodynamic studies of adsorption of strontium from aqeous solutions onto low cost rice straw based carbons. *Carbon Science and Technology* 1: 144-153. Retrieved on January 16th, 2018 from http://www.applied-science-innovation.com

Yusuf- Alaya, S. (2014). Synthesis, intercalation and characterization of zeolite A for adsorption studies of methylene blue. A Master's Thesis, Federal University of Technology, Minna, Niger state, Nigeria